Supporting Information

Computationally predicted high throughput free energy phase diagrams for the discovery of solid-state hydrogen storage reactions

Jacob M. Clary,[1] Aaron M. Holder,[1,2,3] Charles B. Musgrave[*,1,2,4,5,6]

[1]Department of Chemical and Biological Engineering, University of Colorado Boulder, Boulder, CO 80309, USA
[2]Materials and Chemical Science and Technology Center, National Renewable Energy Laboratory, Golden, CO 80401, USA
[3]Renewable and Sustainable Energy Institute, University of Colorado Boulder, Boulder, CO 80309, USA
[4]Department of Chemistry, University of Colorado Boulder, Boulder, CO 80309, USA
[5]Renewable and Sustainable Energy Institute, University of Colorado Boulder, Boulder, CO 80309, USA
[6]Materials Science and Engineering Program, University of Colorado Boulder, Boulder, CO 80309, USA

[*]Correspondence and should be addressed to charles.musgrave@colorado.edu

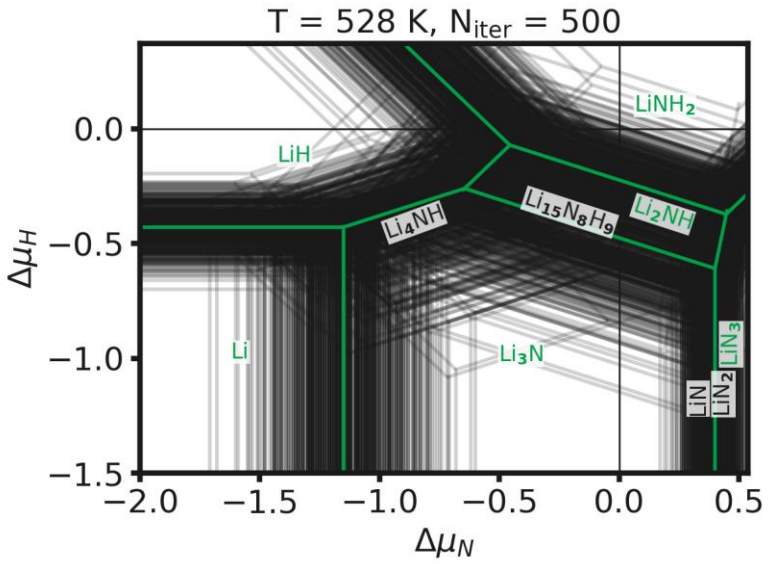

Figure S1. Li-N-H chemical potential phase diagram boundaries at 528 K after applied normally distributed shifts to all ΔH_f and $G^{\delta}(T)$ for 500 iterations. The phase boundaries and associated phases without any applied noise are overlaid in green. The phase boundaries and additional phases that can form due to the introduction of noise are shown in black. The random noise applied here represents the worst case if the errors between compounds in the same compositional space are not correlated and thus shows that the qualitative trends predicted here are likely accurate. Regions of stability for the Li, LiH, Li_3N, and $LiNH_2$ phases were always present. Regions of stability for the LiN_3, Li_2NH, LiN_2, Li_4NH, $Li_{15}N_8H_9$, and LiN phases were present in 81.0%, 74.6%, 33.0%, 32.0%, 21.6%, and 0.2% of iterations. We note that the $Li_{15}N_8H_9$ phase is a mixed $Li_2NH/LiNH_2$ phase with a crystal structure most similar to the Li_2NH phase. Because the $Li_2NH/LiNH_2$ mixed phases in this compositional space can be written as $Li_{2x+y}(NH)_x(NH_2)_y$, the $Li_{15}N_8H_9$ phase is more accurately represented as $Li_{15}(NH)_7(NH_2)$ (x = 7 and y = 1). Because the errors associated with describing this phase are expected to be highly correlated with the error in Li_2NH due to their crystal structure similarity, the shifts applied to this phase were calculated via a linear weighting, determined by x and y, of the shifts applied to Li_2NH and $LiNH_2$. Thus, a Li_2NH-like phase was present in 96.2% of iterations.

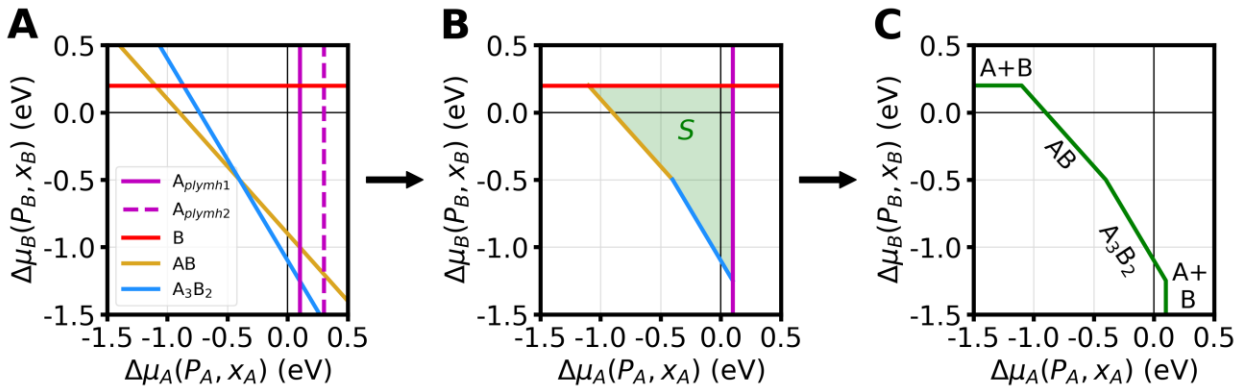

Figure S2. Example schematic for constructing chemical potential phase diagram for binary A-B compositional space. This compositional space contains two polymorphs of element A, element B, and the compounds AB and A_3B_2. **A)** Lines defined by Eq. 2 and 3 for all species. **B)** Largest shape S bounded by the lowest energy polymorphs of all Eq. 2 and 3. **C)** Regions over $\Delta\mu_A(P_A, x_A)$ where each species is stable. Note that for two polymorphs of compound AB, which we call AB_{p1} and AB_{p2}, the polymorph with more negative ΔG_f will be the thermodynamically favored compound. Mathematically, this is equivalent to writing: $\Delta G_{f,AB_{p1}} = \Delta\mu_A(P_A, x_A) + \Delta\mu_B(P_B, x_B)$ and $\Delta G_{f,AB_{p2}} = \Delta\mu_A(P_A, x_A) + \Delta\mu_B(P_B, x_B)$. Rearranging both equations for

$\Delta\mu_A(P_A, x_A)$ and solving for the compound with minimum $\Delta\mu_B(P_B, x_B)$ at all independent $\Delta\mu_A(P_A, x_A)$ results in predicting the most stable polymorph of AB and the one with most negative ΔG_f. This process can be repeated for any number of phases within the compositional space.

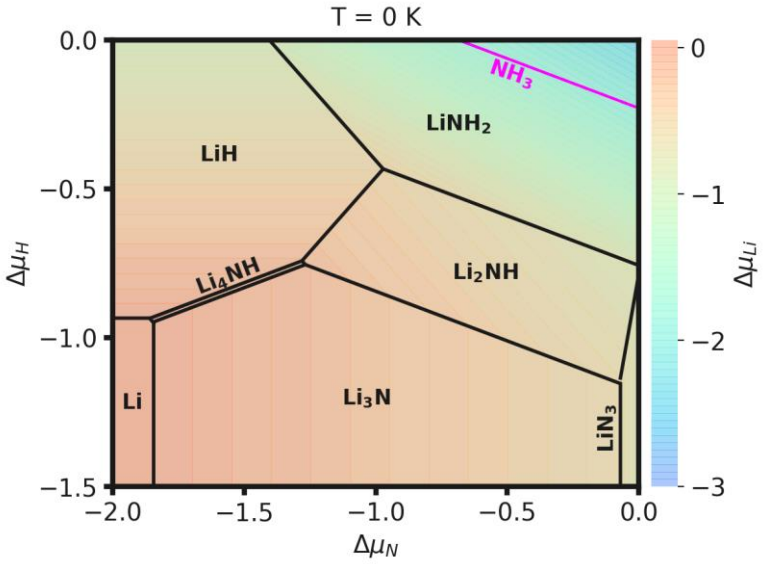

Figure S3. Li-N-H ternary chemical potential phase diagram. At T = 0 K. The regions labeled by compositions are regions of stability for compounds with those compositions. The sets of $\Delta\mu_i$ that fall above the magenta line correspond to conditions where NH_3 is predicted to be stable.

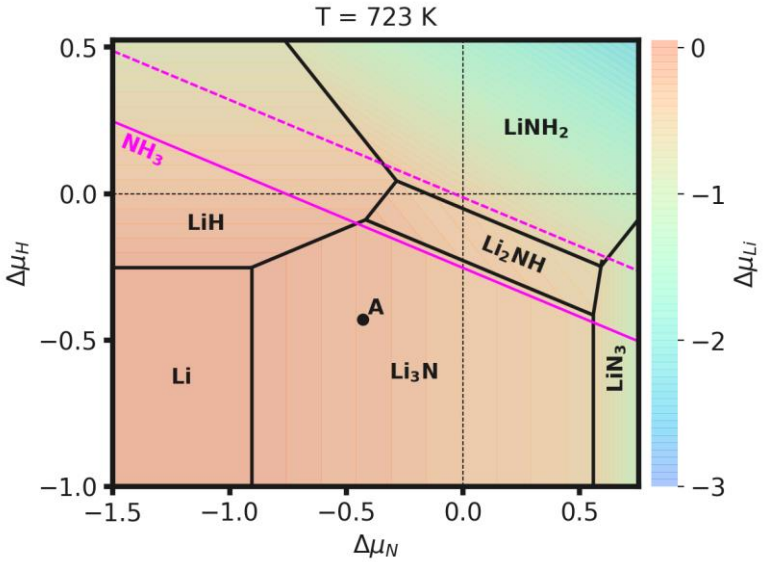

Figure S4. Li-N-H ternary chemical potential phase diagram. At T = 723 K. The regions labeled by compositions are regions of stability for compounds with those compositions. The sets of $\Delta\mu_i$ that fall above the magenta lines correspond to conditions where NH_3 is predicted to be stable for $P_{NH_3} = 10^{-6}\ bar$ (solid) and $P_{NH_3} = 0.1\ bar$ (dashed). The black point labeled A corresponds to conditions of vacuum P_{N_2} and P_{H_2} ($\Delta\mu_N = \Delta\mu_H = -0.43\ eV$).

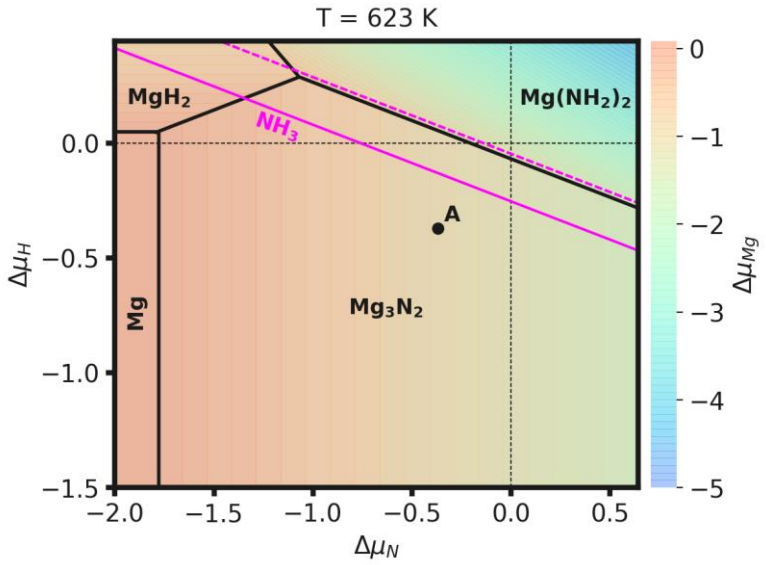

Figure S5. Mg-N-H ternary chemical potential phase diagram. At T = 623 K. The regions labeled by compositions are regions of stability for compounds with those compositions. The sets of $\Delta\mu_i$ that fall above the magenta lines correspond to conditions where NH_3 is predicted to be stable for $P_{NH_3} = 10^{-6}\ bar$ (solid) and $P_{NH_3} = 0.1\ bar$ (dashed). The black point labeled A corresponds to conditions of vacuum P_{N_2} and P_{H_2} ($\Delta\mu_N = \Delta\mu_H = -0.37\ eV$).

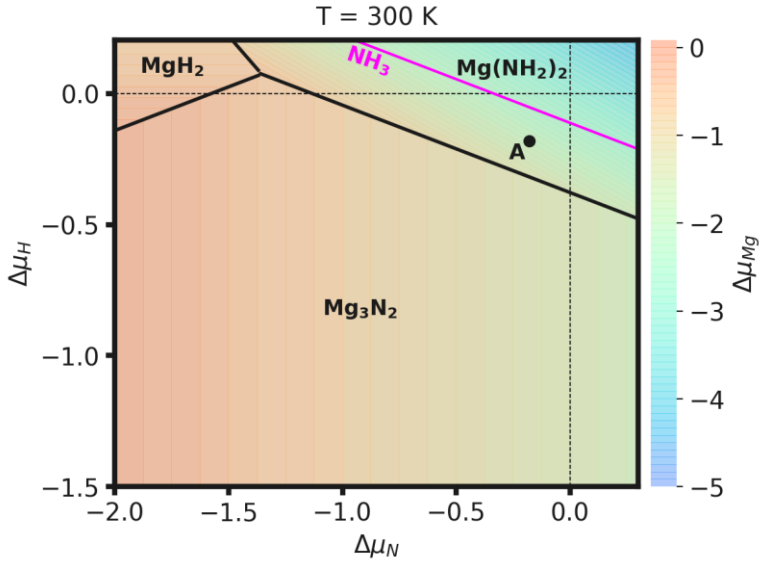

Figure S6. Mg-N-H ternary chemical potential phase diagram. At T = 300 K. The regions labeled by compositions are regions of stability for compounds with those compositions. The sets of $\Delta\mu_i$ that fall above the magenta line correspond to conditions where NH_3 is predicted to be stable for $P_{NH_3} = 5\ bar$. The black point labeled A corresponds to conditions of vacuum P_{N_2} and P_{H_2} ($\Delta\mu_N = \Delta\mu_H = -0.18\ eV$).

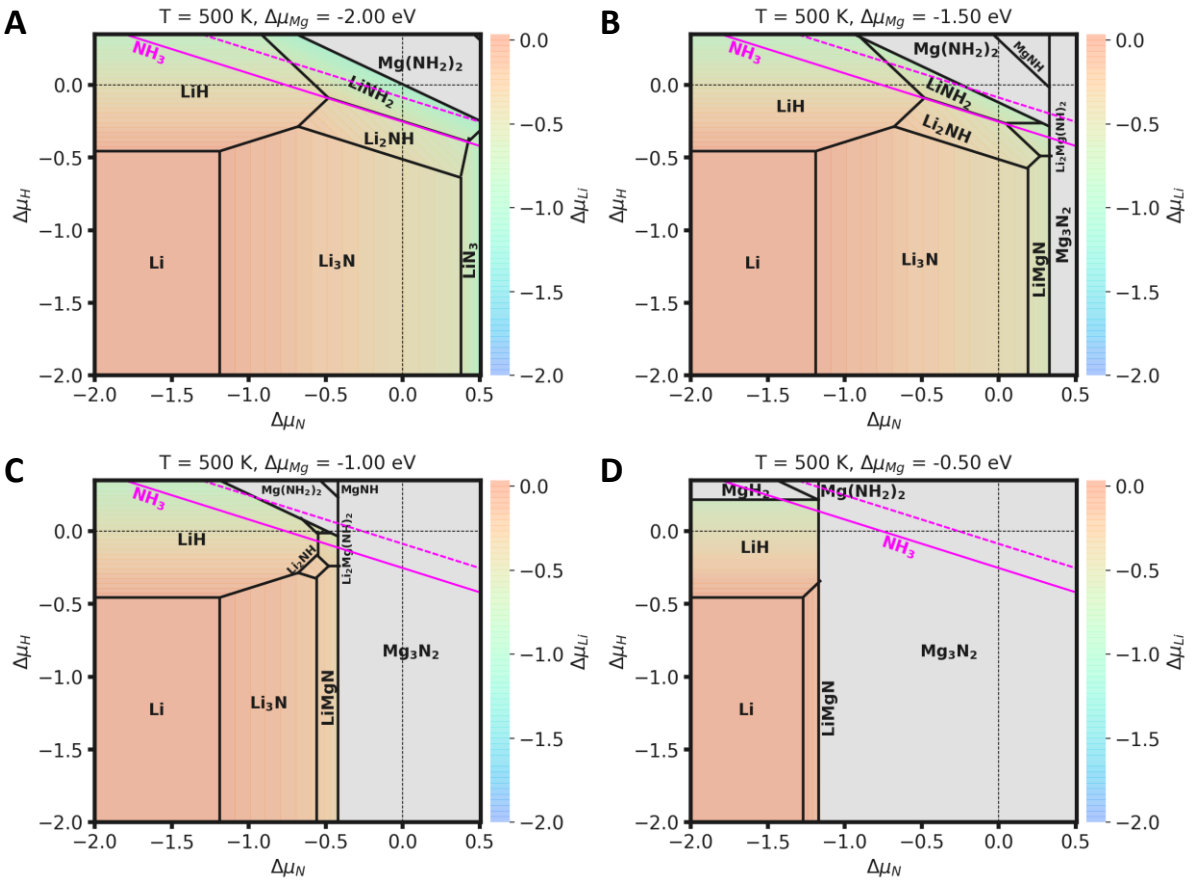

Figure S7. Li-Mg-N-H quaternary chemical potential phase diagram. At T = 500 K. **A)** $\Delta\mu_{Mg} = -2.00\ eV$, **B)** $\Delta\mu_{Mg} = -1.50\ eV$, **C)** $\Delta\mu_{Mg} = -1.00\ eV$, and **D)** $\Delta\mu_{Mg} = -0.50\ eV$. The regions labeled by compositions are regions of stability for compounds with those compositions. The sets of $\Delta\mu_i$ that fall above the magenta lines correspond to conditions where NH_3 is predicted to be stable for $P_{NH_3} = 10^{-6}\ bar$ (solid) and $P_{NH_3} = 0.1\ bar$ (dashed).

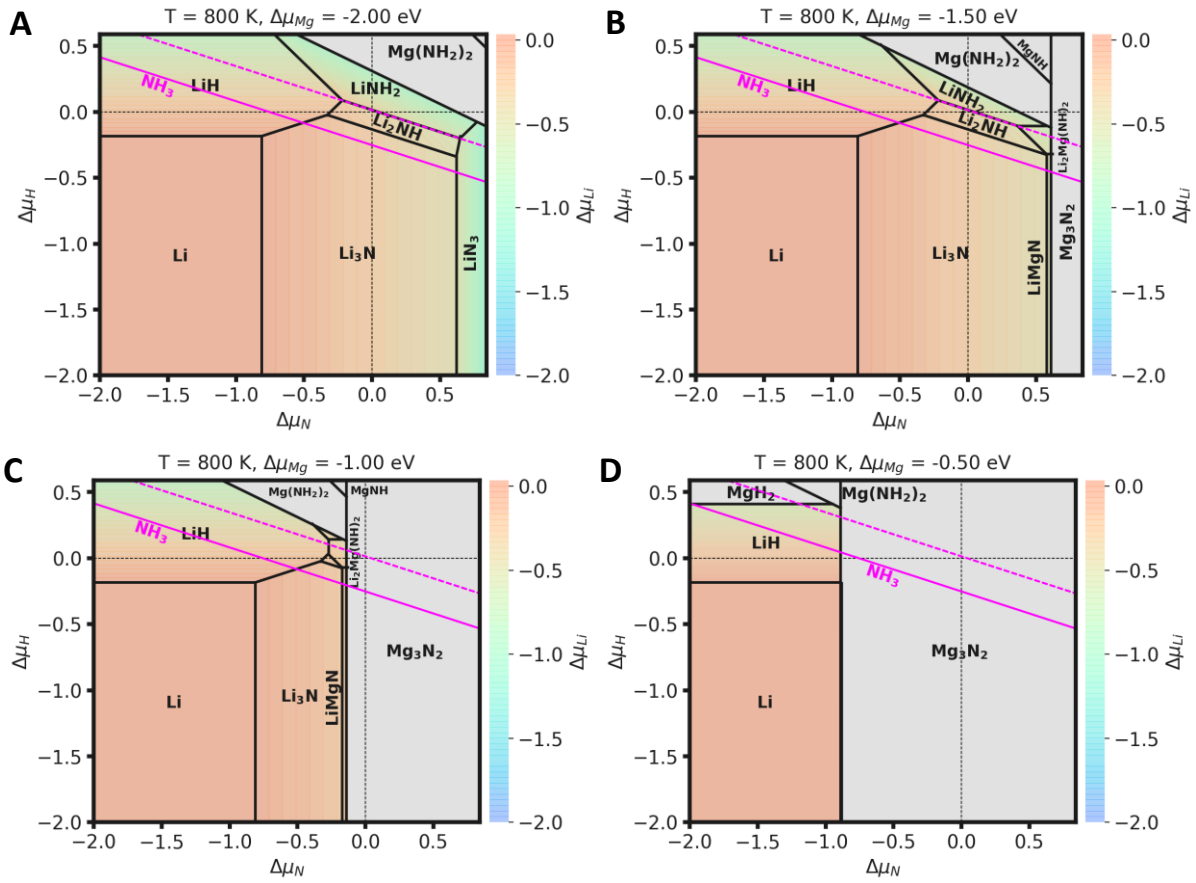

Figure S8. Li-Mg-N-H quaternary chemical potential phase diagram. At T = 800 K. **A)** $\Delta\mu_{Mg} = -2.00\ eV$, **B)** $\Delta\mu_{Mg} = -1.50\ eV$, **C)** $\Delta\mu_{Mg} = -1.00\ eV$, and **D)** $\Delta\mu_{Mg} = -0.50\ eV$. The regions labeled by compositions are regions of stability for compounds with those compositions. The sets of $\Delta\mu_i$ that fall above the magenta lines correspond to conditions where NH_3 is predicted to be stable for $P_{NH_3} = 10^{-6}\ bar$ (solid) and $P_{NH_3} = 0.1\ bar$ (dashed).

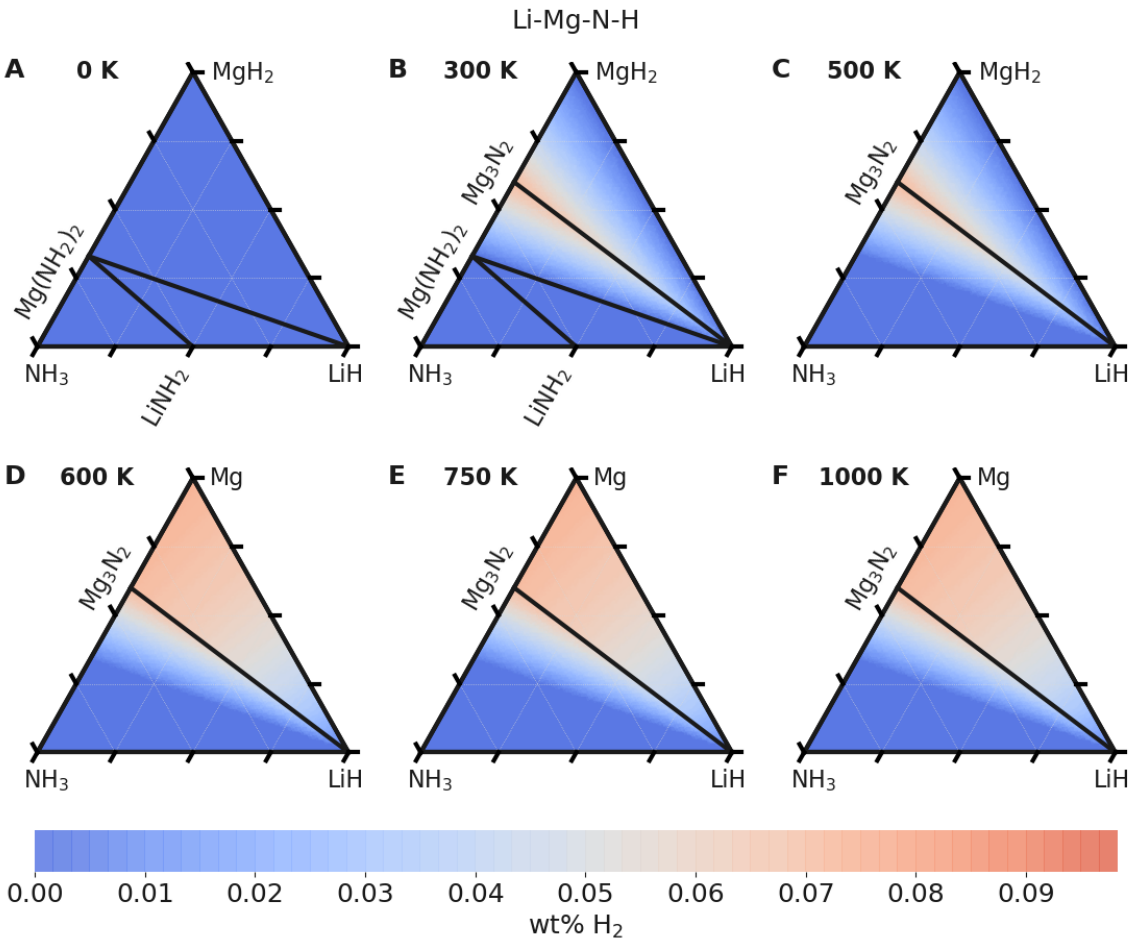

Figure S9. Composition phase diagrams of Li-Mg-N-H system at different temperatures at $P_{NH_3} = 10^{-6}\ bar$. A) 0 K, **B)** 300 K, **C)** 500 K, **D)** 600 K, **E)** 750 K, **F)** 1000 K. The color axis is the weight fraction of released H_2 relative to the mixture at 0 K.

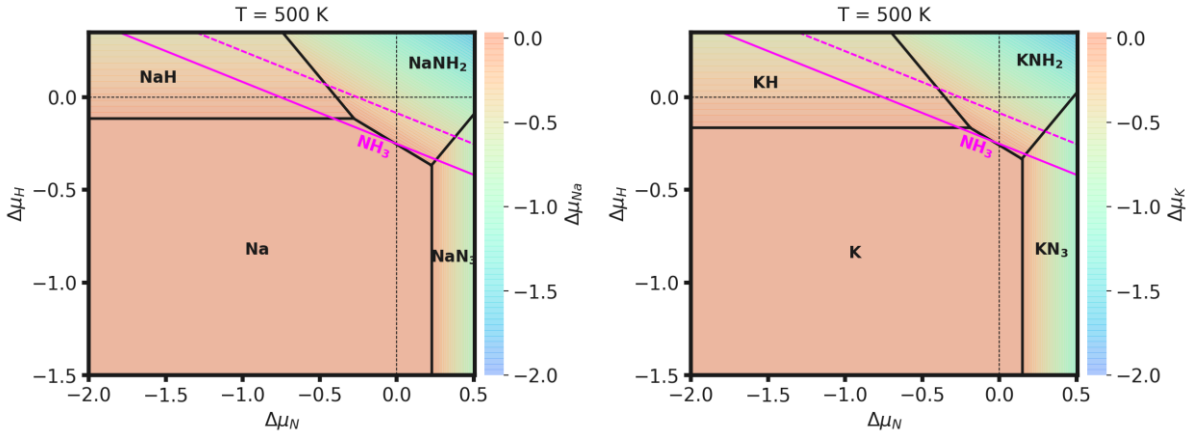

Figure S10. Alk-N-H ternary chemical potential phase diagrams. At T = 500 K. The regions labeled by compositions are regions of stability for compounds with those compositions. The sets of $\Delta\mu_i$ that fall above the magenta lines correspond to conditions where NH_3 is predicted to be stable for $P_{NH_3} = 10^{-6}\ bar$ (solid) and $P_{NH_3} = 0.1\ bar$ (dashed).

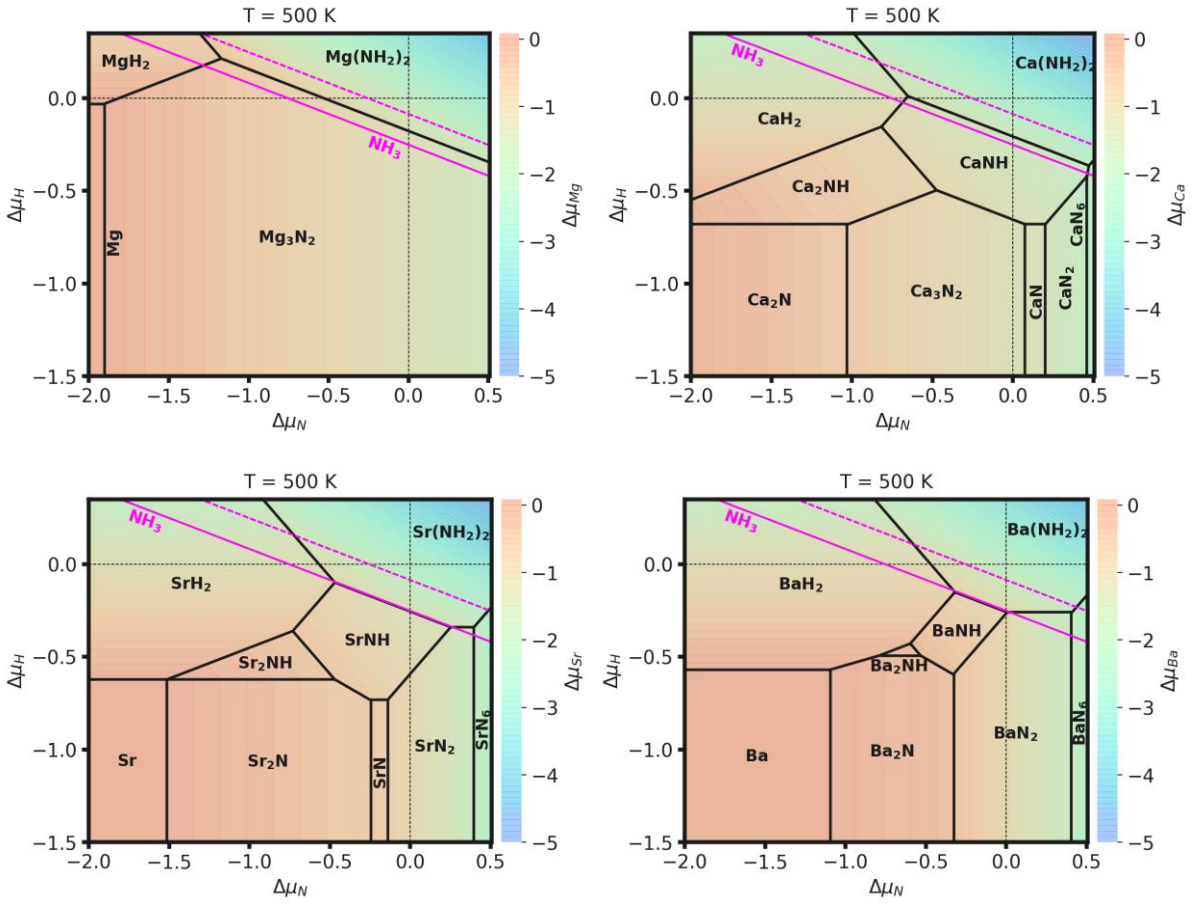

Figure S11. AE-N-H chemical potential ternary phase diagrams. At T = 500 K. The regions labeled by compositions are regions of stability for compounds with those compositions. The sets of $\Delta\mu_i$ that fall above the magenta lines correspond to conditions where NH_3 is predicted to be stable for $P_{NH_3} = 10^{-6}\ bar$ (solid) and $P_{NH_3} = 0.1\ bar$ (dashed).

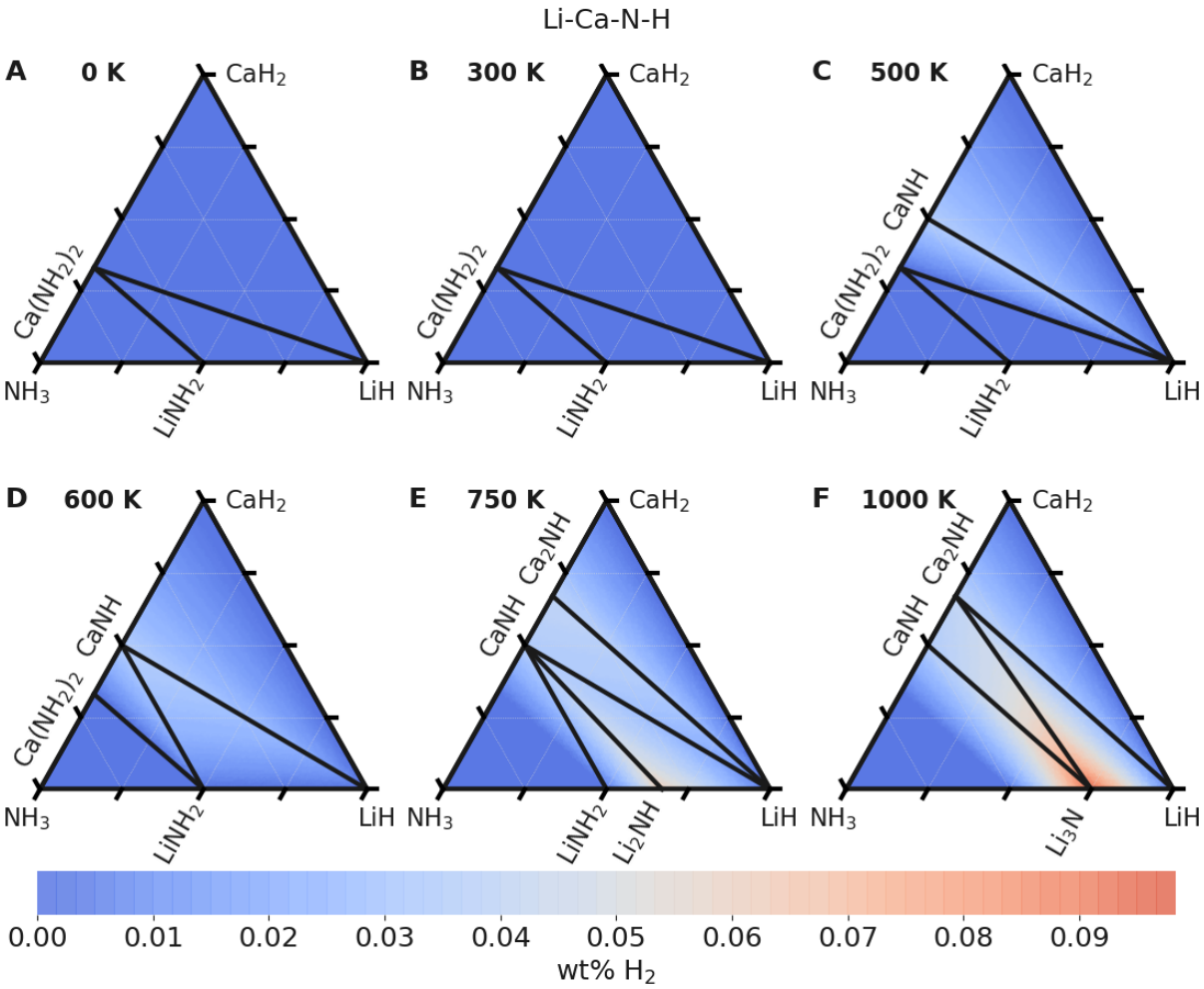

Figure S12. Composition phase diagrams of Li-Ca-N-H system at different temperatures at $P_{NH_3} = 0.1\ bar$. A) 0 K, **B)** 300 K, **C)** 500 K, **D)** 600 K, **E)** 750 K, **F)** 1000 K. The color axis is the weight fraction of released H_2 relative to the mixture at 0 K.

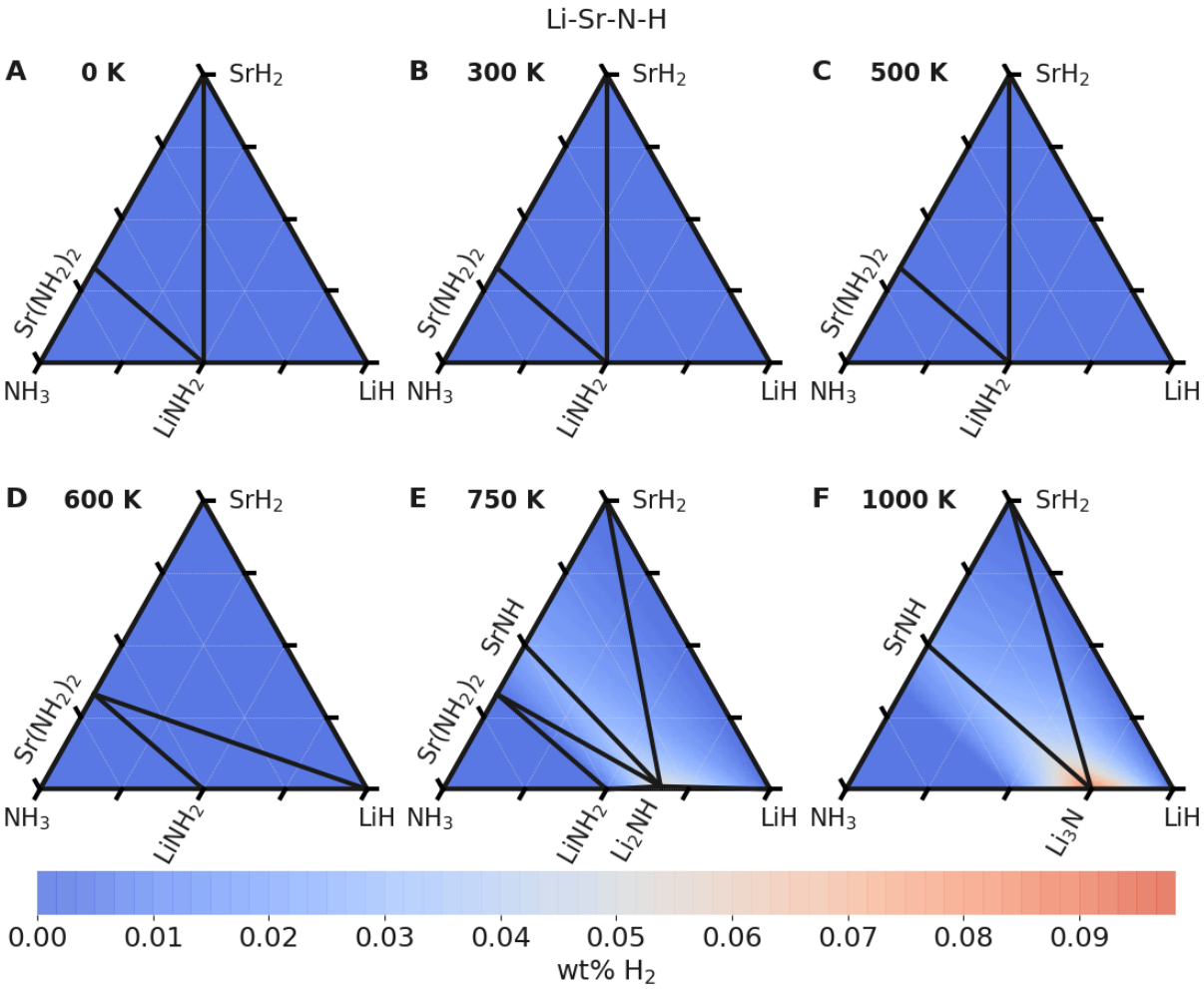

Figure S13. Composition phase diagrams of Li-Sr-N-H system at different temperatures at $P_{NH_3} = 0.1\ bar$. A) 0 K, **B)** 300 K, **C)** 500 K, **D)** 600 K, **E)** 750 K, **F)** 1000 K. The color axis is the weight fraction of released H_2 relative to the mixture at 0 K.

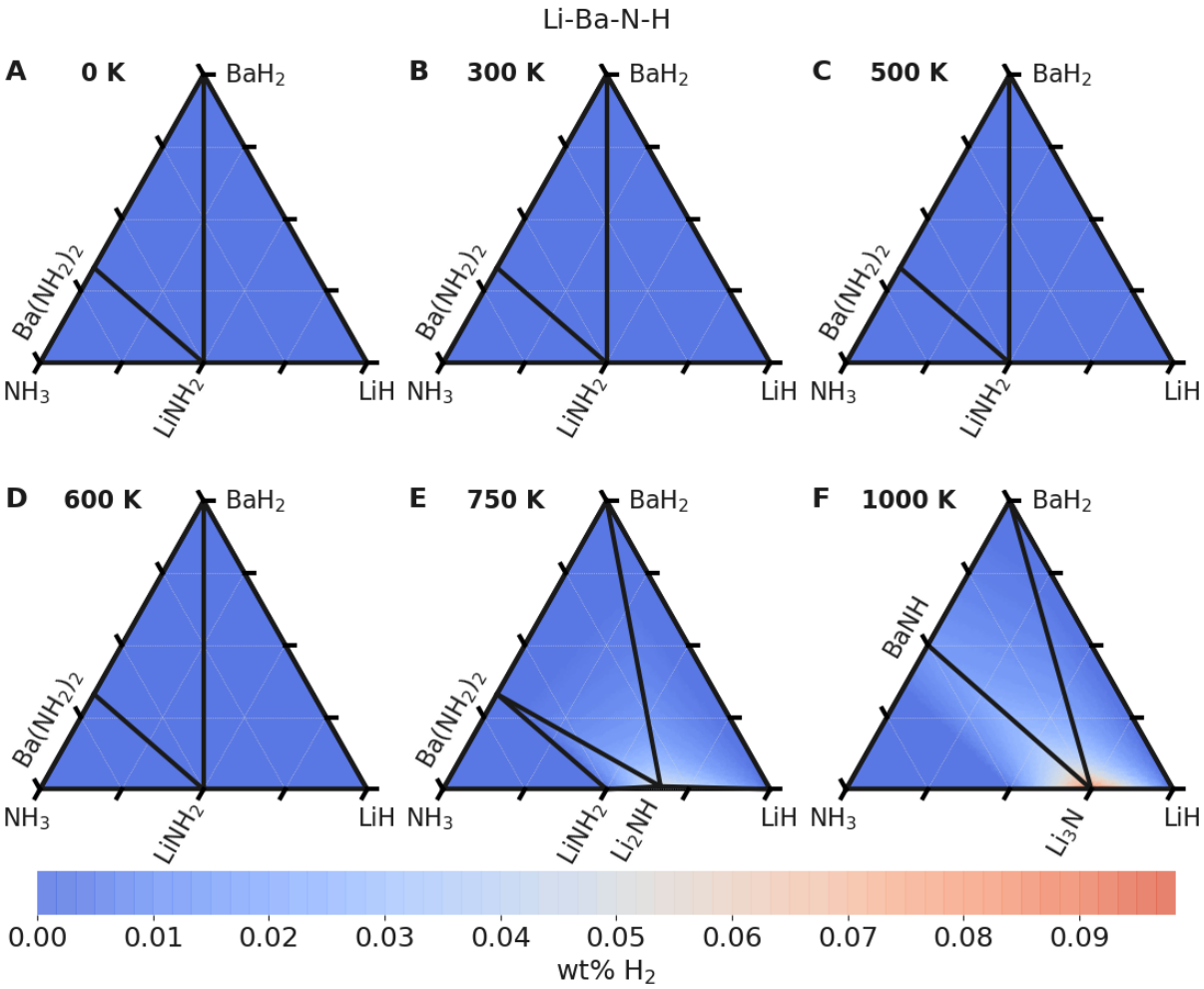

Figure S14. Composition phase diagrams of Li-Ba-N-H system at different temperatures at $P_{NH_3} = 0.1\ bar$. A) 0 K, **B)** 300 K, **C)** 500 K, **D)** 600 K, **E)** 750 K, **F)** 1000 K. The color axis is the weight fraction of released H_2 relative to the mixture at 0 K.

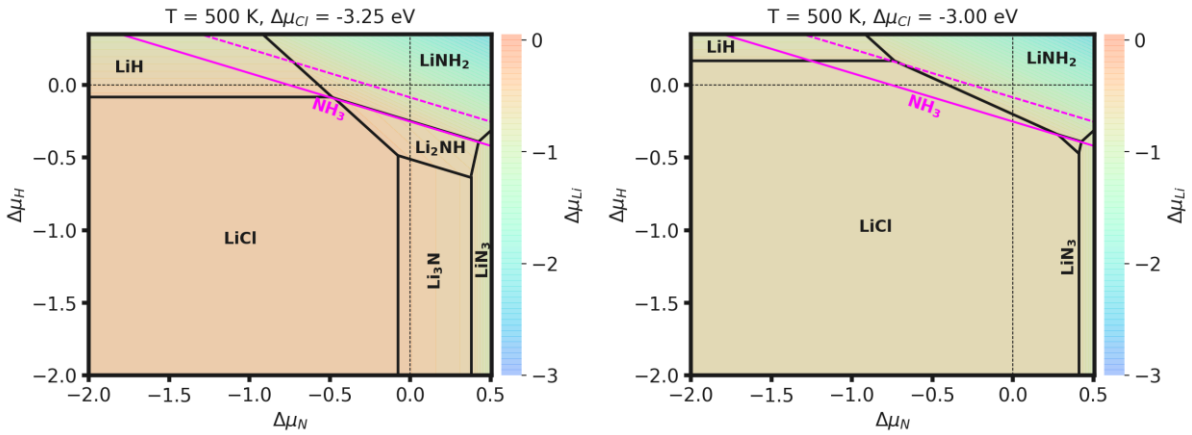

Figure S15. Li-Cl-N-H quaternary chemical potential phase diagram. At T = 500 K. The regions labeled by compositions are regions of stability for compounds with those compositions. The sets of $\Delta\mu_i$ that fall above the magenta lines correspond to conditions where NH_3 is predicted to be stable for $P_{NH_3} = 10^{-6}\ bar$ (solid) and $P_{NH_3} = 0.1\ bar$ (dashed).

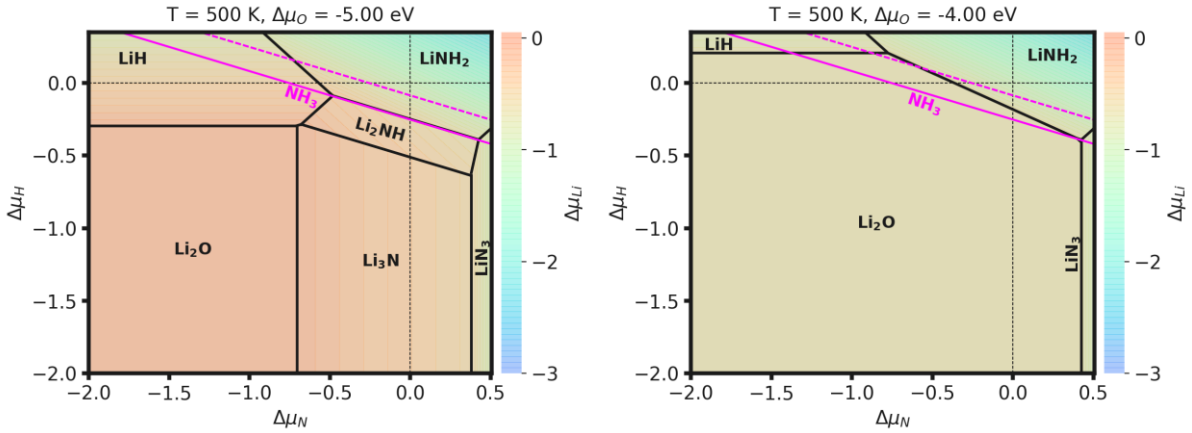

Figure S16. Li-O-N-H quaternary chemical potential phase diagram. At T = 500 K. The regions labeled by compositions are regions of stability for compounds with those compositions. The sets of $\Delta\mu_i$ that fall above the magenta lines correspond to conditions where NH_3 is predicted to be stable for $P_{NH_3} = 10^{-6}\ bar$ (solid) and $P_{NH_3} = 0.1\ bar$ (dashed).

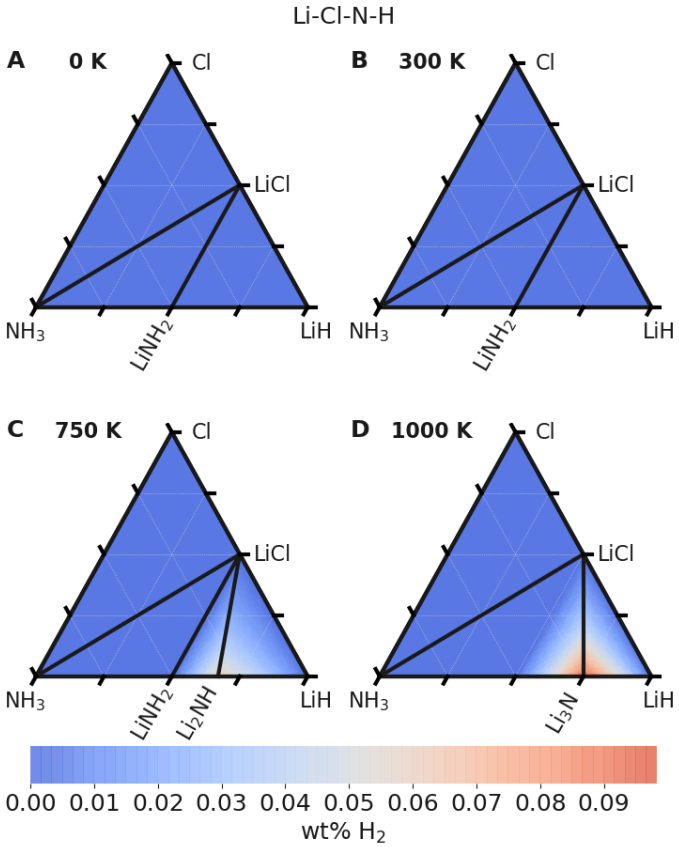

Figure S17. Composition phase diagrams of Li-Cl-N-H system at different temperatures at $P_{NH_3} = 0.1\ bar$. A) 0 K, **B)** 300 K, **C)** 750 K, **D)** 1000 K. The color axis is the weight fraction of released H_2 relative to the mixture at 0 K.

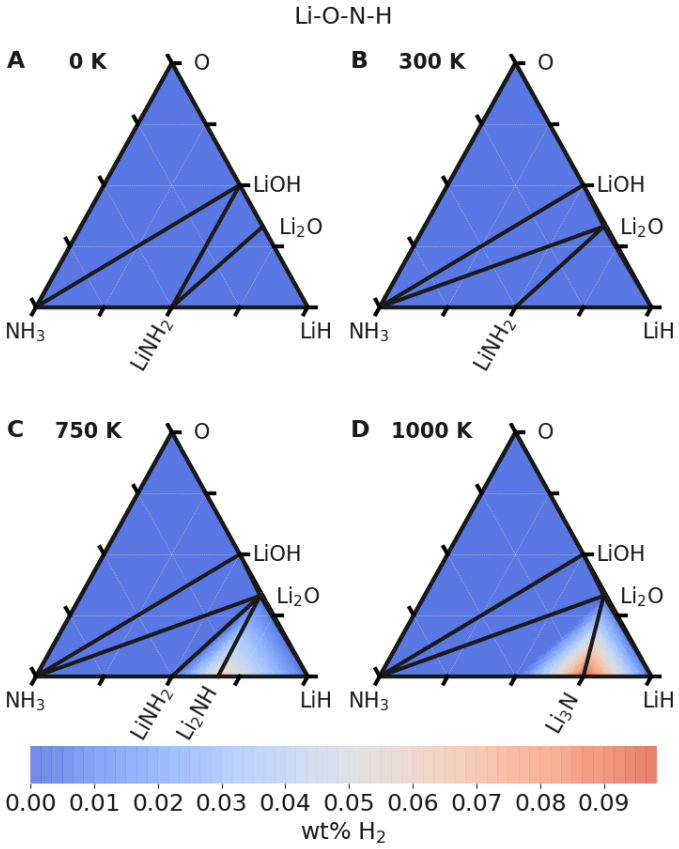

Figure S18. Composition phase diagrams of Li-O-N-H system at different temperatures at $P_{NH_3} = 0.1\ bar$. A) 0 K, **B)** 300 K, **C)** 750 K, **D)** 1000 K. The color axis is the weight fraction of released H_2 relative to the mixture at 0 K.

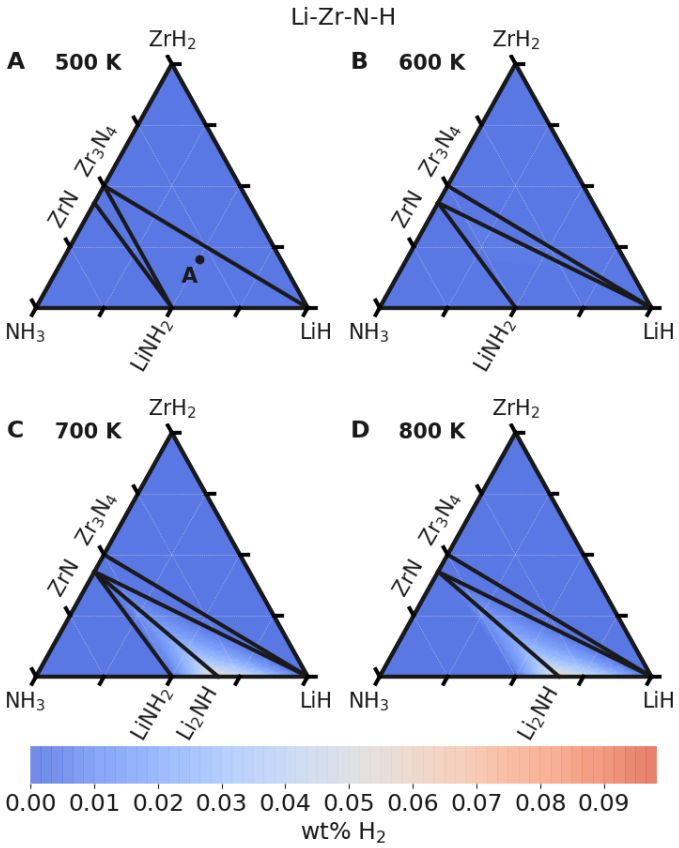

Figure S19. Composition phase diagrams of Li-Zr-N-H system at different temperatures at $P_{NH_3} = 0.1\ bar$. A) 500 K, **B)** 600 K, **C)** 700 K, **D)** 800 K. The color axis is the weight fraction of released H_2 relative to the mixture at 0 K.

Table S1. PAW pseudopotentials used for all elements.

Element	PAW pseudopotential used
Li	Li
Na	Na_pv
K	K_sv
Mg	Mg
Ca	Ca_sv
Sr	Sr_sv
Ba	Ba_sv
N	N
O	O
H	H
Cl	Cl
Zr	Zr_sv

Derivation of Eq. 4 in Methods section for chemical potential phase diagrams

For any closed *N*-element compositional space at equilibrium, the system's free energy is constant and so the definition of the chemical potential can be used to write the molar Gibbs free energy of any formed compound $G_{A_{\alpha_1}B_{\alpha_2}\ldots}$:

$$G_{A_{\alpha_1}B_{\alpha_2}\ldots} = \sum_i \alpha_i \mu_i \tag{S1}$$

where α_i is the stoichiometric coefficient of each element i in the compound. Because μ_i is the elemental reference state chemical potential ($\mu_i^0(0\ K, 0\ bar)$) plus the deviation from that state ($\Delta\mu_i$), $G_{A_{\alpha_1}B_{\alpha_2}\ldots}$ of any compound at equilibrium, can be written as:

$$G_{A_{\alpha_1}B_{\alpha_2}\ldots} = \sum_i \alpha_i (\mu_i^0 + \Delta\mu_i) \tag{S2}$$

where α_i is the stoichiometric coefficient of each element i in the compound, and each elemental chemical potential μ_i is rewritten as the sum of its elemental reference state chemical potential ($\mu_i^0(0\ K, 0\ bar)$) plus the deviation from that state ($\Delta\mu_i$). Changes in $\Delta\mu_i$ caused by each of these system variables can be considered independently. As a result, we decompose each $\Delta\mu_i$ into a temperature dependent component, $\Delta\mu_i(T)$, and a component containing all other contributions to $\Delta\mu_i$, $\Delta\mu_i(\forall C \neq T)$, where C is any other means of changing μ_i of an element from its reference state μ_i^0. Eq. S2 can be expanded into Eq. 1 using the term definitions described in the Methods.

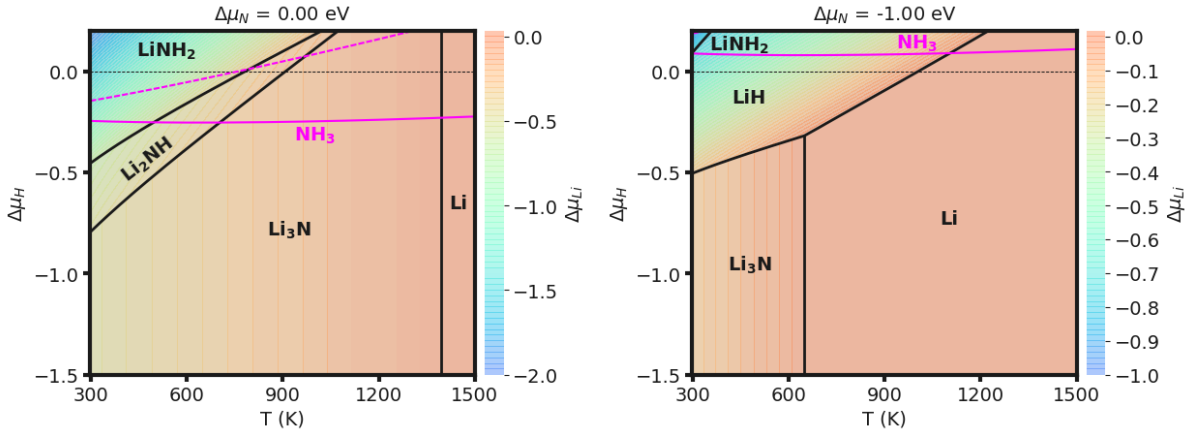

Figure S20. Li-N-H ternary T-$\Delta\mu_H$ phase diagram. The regions labeled by compositions are regions of stability for compounds with those compositions. The sets of $(T, \Delta\mu_i)$ that fall above the magenta lines correspond to conditions where NH_3 is predicted to be stable for $P_{NH_3} = 10^{-6}\ bar$ (solid) and $P_{NH_3} = 0.1\ bar$ (dashed).

Table S2. Zero point energies for gas phase species.

Molecule	ZPE (eV/molecule)
H_2	0.27
N_2	0.15
NH_3	1.79
O_2	0.10
Cl_2	0.03

Table S3. DFT volumes and $\Delta H_f(0\ K)$ for all compounds considered. The MPID is the Materials Project ID number for the compound used as the starting structure for either direct relaxation or structure templating followed by a relaxation.

Index	Formula	MPID	Volume (Å^3/atom)	$\Delta H_f(0\ K)$ (eV/atom)
1	Ba16H1N8	mp-675153	31.76	-0.509
2	Ba1H1N1	mp-34932	17.53	-0.721
3	Ba1H1N1	mp-1187172	17.60	-0.715
4	Ba1H2	mp-23715	18.59	-0.605
5	Ba1H2	mp-1182102	18.60	-0.605
6	Ba1H2	mp-1179094	18.60	-0.605
7	Ba1H2	mp-568441	18.85	-0.582
8	Ba1H2	mp-24809	17.26	-0.579
9	Ba1H2	mp-23759	17.22	-0.579
10	Ba1H2	mp-23711	21.30	-0.561
11	Ba1H4N2	mp-643905	14.14	-0.602
12	Ba1H4N2	mp-696969	14.32	-0.601
13	Ba1H4N2	mp-24383	15.46	-0.544
14	Ba1N1	mp-29973	25.20	-0.581
15	Ba1N2	mp-1001	18.66	-0.650
16	Ba1N2	mp-1009657	18.67	-0.622
17	Ba1N6	mp-1707	16.23	-0.261
18	Ba1N6	mp-2131	17.11	-0.255
19	Ba2H1N1	mp-690794	24.22	-0.629
20	Ba2H1N1	mp-24119	23.98	-0.622
21	Ba2N1	mp-1892	35.50	-0.548
22	Ba3N1	mp-10736	45.76	-0.401
23	Ba3N2	mp-1559	27.78	-0.485
24	Ba3N2	mp-568293	25.61	-0.485
25	Ba3N2	mp-568172	27.52	-0.477
26	Ba3N2	mp-1047	26.84	-0.463
27	Ba3N2	mp-13146	26.12	-0.445
28	Ba8H3N4	mp-530696	25.85	-0.592
29	Ca16H1N8	mp-675153	21.78	-0.878
30	Ca1H1N1	mp-1187172	11.29	-0.943
31	Ca1H1N1	mp-34932	11.72	-0.898
32	Ca1H2	mp-1179094	11.82	-0.663
33	Ca1H2	mp-1102038	13.27	-0.637
34	Ca1H2	mp-568441	12.58	-0.627

35	Ca1H2	mp-23759	11.11	-0.603
36	Ca1H2	mp-23710	15.74	-0.537
37	Ca1H4N2	mp-643905	9.56	-0.700
38	Ca1H4N2	mp-696969	9.69	-0.697
39	Ca1H4N2	mp-24383	12.17	-0.628
40	Ca1N1	mp-29973	17.51	-0.853
41	Ca1N2	mp-1001	12.85	-0.653
42	Ca1N2	mp-1009657	12.68	-0.645
43	Ca1N6	mp-2131	13.06	-0.242
44	Ca1N6	mp-1707	12.71	-0.214
45	Ca2H1N1	mp-690794	15.94	-0.946
46	Ca2H1N1	mp-24119	15.93	-0.942
47	Ca2N1	mp-1892	23.91	-0.886
48	Ca3N1	mp-10736	29.24	-0.632
49	Ca3N2	mp-986716	18.56	-0.959
50	Ca3N2	mp-844	18.56	-0.959
51	Ca3N2	mp-1047	18.14	-0.942
52	Ca3N2	mp-568293	17.45	-0.927
53	Ca3N2	mp-568172	17.16	-0.920
54	Ca3N2	mp-13146	17.17	-0.870
55	Ca8H3N4	mp-530696	17.21	-0.918
56	K15H9N8	mp-1201065	19.36	-0.169
57	K1H1	mp-24721	22.29	-0.296
58	K1H1	mp-24084	22.30	-0.296
59	K1H1	mp-23870	22.32	-0.296
60	K1H2N1	mp-697144	12.90	-0.445
61	K1H2N1	mp-1105785	12.06	-0.433
62	K1H2N1	mp-1079418	12.17	-0.433
63	K1H2N1	mp-1106045	12.24	-0.429
64	K1H2N1	mp-23850	14.41	-0.423
65	K1H2N1	mp-1087524	12.49	-0.422
66	K1H2N1	mp-1189646	12.76	-0.415
67	K1H2N1	mp-23702	17.30	-0.386
68	K1N3	mp-743	15.99	-0.232
69	K1N3	mp-1066400	19.97	-0.206
70	K1N3	mp-581833	16.81	-0.205
71	K1N3	mp-570538	19.09	-0.200
72	K2H1N1	mp-1223097	19.55	-0.126
73	K2H1N1	mp-34465	20.02	-0.120
74	K3H3N2	mp-977164	18.00	-0.269
75	K3N1	mp-2251	32.60	0.422
76	K3N1	mp-2341	24.96	0.517
77	K4H1N1	mp-30228	25.80	0.194
78	K7H5N4	mp-1200910	19.34	-0.207
79	Li15H9N8	mp-1201065	7.84	-0.596
80	Li1Cl1	mp-22905	16.52	-2.069
81	Li1Cl1	mp-1185319	20.21	-2.062
82	Li1H1	mp-23870	7.99	-0.467
83	Li1H1	mp-1009220	7.79	-0.229
84	Li1H1N1	mp-1210462	10.09	-0.263
85	Li1H1N1O2	mp-696315	8.10	-0.958
86	Li1H1O1	mp-625998	8.61	-1.674
87	Li1H2N1	mp-23702	7.70	-0.585

88	Li1H2N1	mp-23850	7.72	-0.583
89	Li1H2N1	mp-1079418	7.36	-0.567
90	Li1H2N1	mp-1188477	7.35	-0.559
91	Li1H2N1	mp-1106045	7.47	-0.548
92	Li1H2N1	mp-1189646	7.26	-0.510
93	Li1H2N1	mp-24428	7.23	-0.492
94	Li1H2N1	mp-1087524	8.00	-0.480
95	Li1H2N1	mp-1188218	7.23	-0.392
96	Li1H2N1	mp-1188409	6.13	-0.358
97	Li1H2N1O3	mp-722902	9.91	-1.044
98	Li1H3	mp-1184938	4.87	0.582
99	Li1H3O2	mp-625211	7.31	-1.400
100	Li1H6N1O6	mp-23906	8.64	-1.064
101	Li1Mg1H6N3	mp-720856	7.51	-0.550
102	Li1Mg1H6N3	mp-696329	7.74	-0.538
103	Li1Mg1N1	mp-37906	10.08	-0.817
104	Li1Mg1N1	mp-30156	10.23	-0.816
105	Li1N1	mp-1179882	9.11	-0.233
106	Li1N1	mp-1180489	9.25	-0.148
107	Li1N1	mp-1064647	7.25	-0.070
108	Li1N1	mp-1059612	7.76	0.813
109	Li1N1	mp-1064119	8.23	0.964
110	Li1N1	mp-1058689	8.49	1.135
111	Li1N1O3	mp-8180	9.27	-1.044
112	Li1N2	mp-1206884	9.62	-0.242
113	Li1N2	mp-1071868	8.42	0.053
114	Li1N3	mp-570538	10.47	-0.203
115	Li1N3	mp-1066400	10.74	-0.198
116	Li1N3	mp-827	10.34	-0.098
117	Li1N3	mp-22777	11.48	0.966
118	Li1N3	mp-1064272	12.08	0.990
119	Li1N3	mp-634410	10.62	1.040
120	Li1N3	mp-636056	13.38	1.074
121	Li1N3	mp-1065265	7.91	1.479
122	Li1N3	mp-1064161	7.19	2.371
123	Li1O2	mp-1018789	8.94	-1.035
124	Li2H1N1	mp-1189725	8.22	-0.602
125	Li2H1N1	mp-699284	7.69	-0.596
126	Li2H1N1	mp-1190219	7.68	-0.575
127	Li2H1N1	mp-34465	7.83	-0.539
128	Li2Mg1H2N2	mp-1193106	8.90	-0.719
129	Li2Mg1H8N4	mp-759183	8.44	-0.559
130	Li2N1	mp-1062345	9.30	-0.176
131	Li2O1	mp-1960	7.96	-2.026
132	Li2O1	mp-755894	7.54	-1.938
133	Li2O2	mp-841	7.93	-1.601
134	Li3H2N2	mp-1210795	8.34	-0.358
135	Li3H3N2	mp-977164	7.99	-0.571
136	Li3N1	mp-999496	10.88	-0.462
137	Li3N1	mp-1190632	8.42	-0.456
138	Li3N1	mp-1189035	8.41	-0.456
139	Li3N1	mp-2639	14.42	-0.449
140	Li3N1	mp-999495	7.62	-0.320

141	Li3N1	mp-11801	15.87	-0.135
142	Li3N2	mp-1222421	11.20	0.302
143	Li4H1N1	mp-30228	9.56	-0.466
144	Li7H5N4	mp-1200910	7.92	-0.592
145	Mg16H1N8	mp-675153	14.17	-0.668
146	Mg1H1N1	mp-1187172	8.34	-0.718
147	Mg1H1N1	mp-34932	8.29	-0.601
148	Mg1H2	mp-23710	9.91	-0.269
149	Mg1H2	mp-23711	9.72	-0.267
150	Mg1H2	mp-1102038	9.01	-0.232
151	Mg1H2	mp-23714	8.00	-0.176
152	Mg1H2	mp-23713	8.00	-0.176
153	Mg1H2	mp-1182102	8.00	-0.176
154	Mg1H2	mp-1181926	8.01	-0.176
155	Mg1H4N2	mp-24383	9.03	-0.619
156	Mg1H4N2	mp-643905	7.05	-0.564
157	Mg1H4N2	mp-696969	7.16	-0.561
158	Mg1Li3H8N4	mp-505381	9.02	-0.501
159	Mg1Li4H10N5	mp-1221143	8.80	-0.518
160	Mg1Li7H16N8	mp-707956	8.49	-0.449
161	Mg1N1	mp-29973	13.30	-0.570
162	Mg1N2	mp-1001	10.39	-0.225
163	Mg1N6	mp-676	10.86	0.059
164	Mg1N6	mp-1707	11.02	0.073
165	Mg2H1N1	mp-690794	10.92	-0.673
166	Mg2H1N1	mp-24119	10.98	-0.664
167	Mg2Li1H2N1	mp-1192182	10.25	-0.537
168	Mg2Li1H6N3	mp-604147	11.36	-0.378
169	Mg2N1	mp-1245	15.19	-0.656
170	Mg3N1	mp-10736	17.60	-0.327
171	Mg3N2	mp-1559	12.11	-0.976
172	Mg3N2	mp-1047	11.83	-0.919
173	Mg3N2	mp-568293	11.49	-0.893
174	Mg3N2	mp-568172	11.38	-0.883
175	Mg3N2	mp-13146	11.30	-0.841
176	Mg8H3N4	mp-530696	11.75	-0.643
177	N1H3	mp-0	330.00	-0.266
178	Na15H9N8	mp-1201065	12.65	-0.270
179	Na1H1	mp-24721	13.41	-0.297
180	Na1H1	mp-23870	13.40	-0.297
181	Na1H2N1	mp-23850	11.13	-0.442
182	Na1H2N1	mp-1079418	9.31	-0.439
183	Na1H2N1	mp-23702	11.71	-0.437
184	Na1H2N1	mp-24428	9.16	-0.434
185	Na1H2N1	mp-1188477	9.28	-0.433
186	Na1H2N1	mp-1106045	8.78	-0.421
187	Na1H2N1	mp-1087524	8.61	-0.417
188	Na1H2N1	mp-1189646	9.24	-0.395
189	Na1N3	mp-570538	13.70	-0.174
190	Na1N3	mp-1066400	13.95	-0.172
191	Na1N3	mp-827	12.11	-0.152
192	Na1N3	mp-581833	12.93	-0.106
193	Na2H1N1	mp-699284	12.69	-0.241

194	Na2H1N1	mp-34465	13.06	-0.217
195	Na3H3N2	mp-977164	12.06	-0.338
196	Na3N1	mp-2251	19.70	0.172
197	Na3N1	mp-2341	15.62	0.214
198	Na4H1N1	mp-30228	16.96	0.031
199	Na7H5N4	mp-1200910	12.78	-0.292
200	Sr16H1N8	mp-675153	26.86	-0.671
201	Sr1H1N1	mp-1187172	13.82	-0.839
202	Sr1H1N1	mp-34932	14.27	-0.818
203	Sr1H2	mp-1182102	14.77	-0.655
204	Sr1H2	mp-1179094	14.74	-0.655
205	Sr1H2	mp-23711	16.66	-0.626
206	Sr1H2	mp-568441	15.11	-0.625
207	Sr1H2	mp-24809	13.84	-0.610
208	Sr1H2	mp-1205322	13.82	-0.610
209	Sr1H4N2	mp-643905	11.45	-0.665
210	Sr1H4N2	mp-696969	11.60	-0.663
211	Sr1H4N2	mp-24383	14.28	-0.582
212	Sr1N1	mp-29973	21.33	-0.686
213	Sr1N2	mp-1001	15.24	-0.650
214	Sr1N2	mp-1009657	15.19	-0.643
215	Sr1N6	mp-2131	14.77	-0.270
216	Sr1N6	mp-1707	14.11	-0.256
217	Sr2H1N1	mp-690794	19.73	-0.772
218	Sr2H1N1	mp-24119	19.63	-0.769
219	Sr2N1	mp-1892	29.61	-0.682
220	Sr3N1	mp-10736	37.16	-0.495
221	Sr3N2	mp-844	23.01	-0.676
222	Sr3N2	mp-1047	22.54	-0.660
223	Sr3N2	mp-568293	21.53	-0.653
224	Sr3N2	mp-568172	21.28	-0.640
225	Sr3N2	mp-13146	21.48	-0.590
226	Sr8H3N4	mp-530696	21.23	-0.739